AEDC-TDR-64-84

TEMPERATURE EFFECTS ON THE CAPTURE COEFFICIENTS OF SIX COMMON GASES

By

J. P. Dawson
Aerospace Environmental Facility
ARO, Inc.

TECHNICAL DOCUMENTARY REPORT NO. AEDC-TDR-64-84

May 1964

Program Element 61405014/8951, Task 895104

(Prepared under Contract No. AF 40(600)-1000 by ARO, Inc., contract operator of AEDC, Arnold Air Force Station, Tenn.)

ARNOLD ENGINEERING DEVELOPMENT CENTER
AIR FORCE SYSTEMS COMMAND
UNITED STATES AIR FORCE

NOTICES

Qualified requesters may obtain copies of this report from DDC, Cameron Station, Alexandria, Va. Orders will be expedited if placed through the librarian or other staff member designated to request and receive documents from DDC.

When Government drawings, specifications or other data are used for any purpose other than in connection with a definitely related Government procurement operation, the United States Government thereby incurs no responsibility nor any obligation whatsoever; and the fact that the Government may have formulated, furnished, or in any way supplied the said drawings, specifications, or other data, is not to be regarded by implication or otherwise as in any manner licensing the holder or any other person or corporation, or conveying any rights or permission to manufacture, use, or sell any patented invention that may in any way be related thereto.

TEMPERATURE EFFECTS ON THE CAPTURE COEFFICIENTS OF SIX COMMON GASES

By

J. P. Dawson

Aerospace Environmental Facility

ARO, Inc.

a subsidiary of Sverdrup and Parcel, Inc.

May 1964

ARO Project No. SW2417

AF - AEDC
Arnold AFS Tenn

ABSTRACT

The effects of gas and cryosurface temperature on the capture coefficient of six gases are discussed. The gas temperature effect is interpreted by the critical velocity model, and the cryosurface temperature effect is qualitatively explained by the potential field model. The possible error involved when these results are extrapolated to higher gas temperatures is also discussed.

Experimental results are presented for the cryopumping rates of nitrogen, argon, carbon monoxide, nitrous oxide, oxygen, and carbon dioxide over 10 to 25°K cryosurfaces and a gas temperature range of from 77 to 400°K.

PUBLICATION REVIEW

This report has been reviewed and publication is approved.

Hans K. Doetsch
H. K. Doetsch
Technical Advisor
DCS/Research

D. R. Eastman, Jr.
Donald R. Eastman, Jr.
DCS/Research

CONTENTS

TABLES

ILLUSTRATIONS

NOMENCLATURE

A_c	Cryosurface area, cm^2
A_j	Recorded peak height of mass spectrometer at mass j, scale divisions
a_{ij}	Mass spectrometer sensitivity for the "i"th component at mass j, scale divisions/mm Hg
C	Capture coefficient
$f(V_x)$	Fraction of molecules with normal velocity in the interval $(V_x, V_x + dV_x)$
k	Boltzmann constant, ergs/°K molecule
M	Molecular weight, grams
m	Weight of molecule, grams
P_c	Chamber pressure, mm Hg
P_o	Forepressure on the standard leak, mm Hg
P_s	Vapor pressure of condensate, mm Hg
R	Universal gas constant, ergs/mole °K
S	Pumping speed, liters/cm^2-sec
T_g	Gas temperature, °K
T_o	Temperature of the standard leaks, °K
T_s	Cryosurface temperature, °K
T_w	Temperature of the shroud liner, °K
$\dot{V}_o$	Volume flow rate through the standard leaks at P_o, T_o, liters/sec
V_x	x-component of velocity, cm/sec
V_{x_o}	Critical x-component of velocity, cm/sec
ϵ	Energy of molecule, ergs/molecule

1.0 INTRODUCTION

This report is a continuation of the experimental program to determine the cryopumping speeds of the gases to be removed from environmental test chambers as a result of space vehicle outgassing, chamber outgassing, and the firing of vehicle control rockets. These data are necessary to help predict the altitude simulation that can be achieved in a space environmental chamber under test conditions (Ref. 1). In order to make these predictions, it is necessary to know the effect of gas temperature, cryosurface temperature, gas compositions, and directed flow on the cryopumping speeds (capture coefficients) of the individual gases. This report investigates the effect of gas and cryosurface temperatures for several gases. Experimental pumping speeds and capture coefficients are presented for 300 and 400°K nitrogen (N_2), argon (A), carbon monoxide (CO), and nitrous oxide (N_2O) and 77°K carbon monoxide over a cryosurface temperature range of from 9.5 to 25°K. Also, capture coefficients are presented for 77, 300, and 400°K oxygen (O_2) which were estimated from experimental pumping speeds of air and N_2-O_2 mixtures (Ref. 2). The experimental data are analyzed employing the critical velocity model (Refs. 3 and 4), and data from previous papers (Refs. 5, 6, and 7) are included to facilitate the explanation of the gas and cryosurface temperature effects. The investigation was conducted in the Ultrahigh Vacuum Chamber, Arnold Engineering Development Center (AEDC), Air Force Systems Command (AFSC).

2.0 APPARATUS

The ultrahigh vacuum chamber (Fig. 1) used in these experiments was designed for a ultimate vacuum in the 10^{-10}-10^{-12} mm Hg pressure range. Since this is the first series of experiments to be conducted in the ultrahigh vacuum chamber, a brief discussion of its performance in addition to a description is given. The chamber is a 60-cm-diam stainless steel cylinder 90 cm in length. The chamber volume after correcting for the cryosphere and shroud volumes is 374 liters. The pumping station for the chamber consists of a 15-cm oil diffusion pump, with both liquid nitrogen and water-cooled baffles. The oil diffusion pump is backed by a 400-liter/min mechanical pump, and the entire pumping system can be isolated from the chamber by a 10-cm high vacuum valve. The chamber is also equipped with a 400-liter/sec VacIon pump which can be isolated by a 15-cm high vacuum valve.

Manuscript received April 1964.

These experiments were conducted in the free-molecular flow regime in which the number of molecule-wall collisions greatly exceeds the number of molecule-molecule collisions. Therefore, the gas temperature will be equal to the shroud temperature (Ref. 8) since the ratio of shroud area to cryosurface area is 24:1. Then the gas temperature may be regulated by proper adjustments of the shroud temperature.

The gas temperature was controlled at 77°K by passing liquid nitrogen through a shroud liner located just inside the chamber wall (Fig. 1). The 300 and 400°K shroud temperatures were obtained by passing air of the desired temperature through the shroud. The temperature of the air was controlled by preheating the air to 25°C above the desired temperature and then circulating it through copper tubing wound around the chamber. External strip heaters on the chamber walls were used to maintain the wall temperature at 300 or 400°K to minimize radiation losses, and the temperature of the air was monitored by thermocouples at the entrance and exit of the shroud. During the actual experiments, the difference between these two temperature measurements was less than 1°C.

The external strip heaters on the chamber walls were also used to outgas the chamber at 550°K; however, the entire system may be outgassed by enclosing it in a removable bakeout oven.

The vacuum chamber contains a 18-cm-diam spherical cryosurface which has an area of 995 cm^2. A helium refrigeration system was employed in controlling the cryosurface temperature from 10 to 30°K, and a helium gas thermometer was used to measure the cryosurface temperature.

The gas addition system is shown in Fig. 2. It consists of five calibrated standard leaks arranged in parallel, and each leak is equipped with a bakeable high vacuum valve. These standard leaks were calibrated by the pressure rise method as described in Ref. 6. The pressure on the high pressure side of the standard leak is controlled by a Granville Phillips, Model B pressure controller which allows the pressure to be maintained within ±0.1 percent of a given pressure setting. The pumping station for the gas addition system consists of a 5-cm oil diffusion pump backed by a 200-liter/sec mechanical pump. The system is also equipped with a bakeout furnace capable of attaining a 550°K bakeout temperature.

The primary measurement of pressure in the ultrahigh vacuum system was made with a calibrated mass spectrometer; however, the chamber was also equipped with a nude ionization gage and a Redhead

vacuum gage for monitoring total chamber pressure. The mass spectrometer and ion gages were calibrated as outlined in Ref. 6.

The pressures attained in the system under various conditions are given in Table 1. The first column indicates the principle component of the gases present in the system before pumpdown from 10^{-5} mm Hg. All pressures were measured with the Redhead vacuum gage, and these pressures were confirmed with the partial pressure analyzer. The background of the analyzer indicated a total pressure in the mass spectrometer tube of 4×10^{-9} mm Hg and consisted mainly of carbon monoxide, mass 28 and water mass 18 in the ratio of approximately 30:1. The low pressures given in Table 1 were therefore not substantiated by mass spectrometer measurements for carbon monoxide. The data presented in Table 1 indicate that the minimum pressure attainable in the ultrahigh vacuum chamber is essentially independent of the gas species present.

Outgassing in a vacuum chamber is dependent on the immediate past history of the system (Ref. 9); however, the rate of pressure rise is still used as an indication of the "tightness" of a system. The actual rate of rise in the ultrahigh vacuum chamber has averaged 2×10^{-11} mm/sec, and the major component was CO, mass 28, which indicates outgassing rather than inleakage from the atmosphere. The important aspect of the low rate of rise is that pumping speed measurements may be made in the 10^{-9}-10^{-10} mm Hg pressure range.

3.0 PROCEDURE

The procedure followed in these measurements in the ultrahigh vacuum chamber was very similar to the procedure employed in previous cryopumping experiments (commonly referred to as the pressure drop method, Refs. 5, 7, and 10).

The experimental conditions desired were obtained by adjustment of the system parameters, i. e., T_g, the gas temperature; T_s, the cryosurface temperature; and V_o, the flow of experimental gas. With the gas temperature (77 to 400°K) and the cryosurface temperature (10 to 30°K) set at the desired level, the experimental gas was introduced through the 10^{-1}-cc/sec standard leak of the gas addition system, coating the cryosurface with the gas condensate. The purpose of this preliminary coating was to eliminate the bare surface effect (Ref. 10). After precoating the cryosurface and with the chamber back to operating conditions (a pressure of 10^{-10} mm Hg), the experimental gas was introduced at a known constant flow rate into the vacuum chamber, and the

system was allowed to reach steady-state conditions. During this phase of the experiment, the only means of removal of gas from the system was the cryosurface since the mechanical pumps were valved off from the system. The constant inleakage rate was accomplished by flowing the experimental gas through a calibrated standard leak and maintaining the back pressure at a known constant value. The back pressure on the standard leak was measured by a mercury manometer and was controlled by a Granville Phillips Model B pressure controller. When the steady-state pressure was reached, as determined by the Redhead vacuum gage, the partial pressure of each gas present was determined by scanning the mass spectrum with the partial pressure analyzer. The flow of gas into the chamber was then stopped by closing a valve in the gas line at the entrance to the chamber, and the system was allowed to reach equilibrium. The partial pressure of the experimental gas at these new chamber conditions was then again determined with the mass spectrometer. This measurement was made to insure that the partial pressure of the experimental gas obtained under inflow condition was caused entirely by the flow through the standard leaks and was not background effects or outgassing. The magnitude of the second measurement was rarely greater than 0.5 percent of the initial measurement.

This procedure was followed in the experiments covering a pressure range of from 10^{-10} to 10^{-5} mm Hg. The pressure drop in the 10^{-10} to 10^{-6} mm Hg pressure range was measured by observing the change in peak height on the mass spectrometer of the parent mass peak for the particular gas in question. The mass spectrometer could not be used for pressure drop measurements above a chamber pressure of 5×10^{-6} mm Hg without exceeding its safe operating limits. The Redhead vacuum gage was used to measure the pressure drop in the 10^{-7} to 10^{-5} mm Hg pressure range. The ratio of experimental gas to impurities in this pressure range was greater than 10^3; therefore, the pressure drop would be essentially caused by removal of experimental gas by cryopumping, and using the Redhead gage for this pressure drop measurement would not introduce any appreciable error. Agreement between the two measurements in the overlap region was very good, better than one percent.

4.0 RESULTS

Cryopumping speeds were determined for 300 and 400°K N_2, A, CO, and N_2O and for 77°K CO on cryosurfaces of from 10 to 25°K. The pumping speeds were calculated (Refs. 5 and 11) from

$$S = \frac{P_o \dot{V}_o a_{ij}}{A_j A_c} \sqrt{\frac{T_w}{T_o}} \qquad (1)$$

where

S is the pumping speed, liters/cm^2-sec

P_o is the forepressure on the standard leak, mm Hg

$\dot{V}_o$ is the volume flow rate through the standard leak at P_o and T_o, liters/sec

A_c is the area of the cryosurface, cm^2

A_j is the recorded peak height of the mass spectrometer at mass j, scale divisions

a_{ij} is the mass spectrometer sensitivity for the "i"th component at mass j, scale divisions/mm Hg

T_w is the temperature of the shroud liner, °K

T_o is the temperature of the mass spectrometer and the standard leaks.

The pumping speeds calculated from these data using Eq. (1) are given in Figs. 3 through 11 and are summarized in Table 2. The pressures given in the figures are the partial pressures of the experimental gas; however, the purity of each gas was such that for all practical purposes the partial pressure of the gas was the total pressure in the vacuum system. Each of the pumping speed values given in Table 2 is the average of from 12 to 24 different measurements which covered the pressure range of from 10^{-9} to 10^{-5} mm Hg. This large number of measurements was made to enable one to make a statistical evaluation of the average error involved in these measurements. From these pumping speed data, the capture coefficient for each gas at each cryosurface temperature was determined. The capture coefficient is defined as (Refs. 6 and 11)

$$C = \frac{S}{\sqrt{RT_g / 2\pi M}\ \left(1 - \frac{P_s}{P_c}\right)} \qquad (2)$$

where

S is the experimental pumping speed, liters/cm^2-sec

R is the universal gas constant, ergs/mole °K

M is the molecular weight of the gas under consideration, grams

T_g is the temperature of the condensable gas, °K

P_s is the vapor pressure of the condensable gas at T_s, mm Hg

P_c is the chamber pressure, mm Hg

Over the stated experimental pressure and cryosurface temperature range, the vapor pressure correction factor, $\left[1 - (P_s/P_c)\right]$, for these experiments is essentially equal to one (Ref. 12) since the ratio of the vapor pressure to the chamber pressure is small. Thus,

$$C = \frac{S}{\sqrt{RT_g/2\pi M}} \tag{3}$$

The values of $\sqrt{RT_g/2\pi M}$, the theoretical maximum pumping speed, for the experimental gases are listed in Table 3 for several gas temperatures. The capture coefficients calculated from Eq. (3) are shown in Figs. 12 through 16 as functions of gas and cryosurface temperatures.

Additional data for 77°K N_2 and A were taken to clarify the change in capture coefficient as a function of cryosurface temperature (Ref. 6). These new data for 77°K N_2 and A are indicated by the flagged symbols in Figs. 12 and 13, respectively. The data points indicated by the circular symbols were obtained in a different research chamber, the trapping chamber, and were reported in Ref. 6. These data are included in this report for the convenience of the reader. The influence of cryosurface and chamber geometry on the capture coefficients has been considered in Refs. 13 and 14, respectively.

An attempt was made to determine the pumping speed of pure 300 and 77°K oxygen; however, the data were inconclusive because of the adverse effect which the oxygen produced on the mass spectrometer. These data indicated that the mass spectrometer sensitivity varied with pressure, and the establishment of steady-state conditions was extremely difficult because of adsorption and desorption from the walls. However, an estimate of the capture coefficient for 77 and 300°K oxygen was made from the cryopumping data obtained on air (Ref. 2). These data are shown graphically in Fig. 18 (see also Section 5.0 for further explanation). The possible error involved in these calculations is considered to be approximately 10 to 12 percent.

A study of the capture coefficients reported in the literature indicates that the capture coefficients measured under the same temperature and pressure conditions by different experimentors yield varying results. This discrepancy in some cases has been as great as from 30 to 50 percent. A possible explanation of these results has been expressed in the literature as a surface effect, which as used in this report may be defined as any change in the capture coefficient or pumping speed that is caused by the physical changes in the condensate. That is, the pumping speed for a 20°K cryosurface could be changed if the initial coating of the surface were made on a 10°K surface rather than a 20°K surface. A series of experiments was made with each experimental gas during the

course of this study to determine if this effect were present. To do this, the initial cryosurface coating was made with the cryosurface at 25°K, and runs were made at 2°K intervals from 25 to 10°K, and then these runs were repeated with the initial coating on a 10°K cryosurface. Also, runs were made when the initial coating and the pumping speed measurements were made at the same cryosurface temperature. No change in the pumping speed greater than the experimental error was observed in any of these runs, and in most cases the difference was less than one percent. It has been concluded from this series of experiments that if such an effect is present, it is smaller than one percent.

5.0 ANALYSIS OF RESULTS

Previous reports (Refs. 5, 6, and 7) have shown that the capture coefficient is a function of the gas and cryosurface temperatures, and the actual capture (Ref. 4) has been determined to be the result of the interaction of the incident molecule with the potential field created by the condensed molecules.

A critical velocity model has been proposed (Refs. 3 and 4) to explain theoretically the effects of gas temperature on the capture coefficient. This velocity model states that all the molecules with a normal velocity less than a critical value, V_{X_O}, will condense on first collision with the cryosurface. This theoretical explanation requires only that Maxwell's law of velocity distribution (Ref. 15) be valid for the experimental system. Since in the experimental system employed in these experiments the ratio of chamber wall area to cryosurface area is quite large, the Maxwellian velocity distribution will not be affected appreciably, and the distribution will be characterized by the chamber wall temperature. Then according to Maxwell's law the fraction of molecules, $f(V_X)$, with velocity components along the x-direction in the interval $(V_X,\ V_X + dV_X)$ is given by (Ref. 15):

$$f(V_x) = \left(\frac{M}{2\pi k T_g}\right)^{1/2} e^{-\frac{MV_x^2}{2kT_g}} \tag{4}$$

Therefore, if a critical velocity, V_{X_O}, exists, the fraction of molecules that would condense is given by

$$C = \frac{\int_0^{V_{x_o}} V_x f(V_x)\, dV_x}{\int_p^{\infty} V_x f(V_x)\, dV_x} \tag{5}$$

where

$$\int_p^{\infty} V_x f(V_x)\, dV_x$$

is the total number of molecules incident on the cryosurface. After substituting for $f(V_x)$ and integrating over the specified limits, one obtains

$$C = 1 - e^{-\frac{MV_{x_o}^2}{2kT_g}} \tag{6}$$

By hypothesis, the quantity $(MV_{x_O}^2)/(2k)$ is a constant for a particular gas; however the effect of cryosurface temperature on V_{x_O} has been neglected.

Examination of the capture coefficients in this report as well as those in the literature indicate that for gas temperatures of 300°K and above, the capture coefficient is mainly a function of the gas temperature. That is,

$$1 - C = e^{-\epsilon/kT_g} \tag{7}$$

This implies that

$$\epsilon = 1/2\, MV_{x_o}^2 \tag{8}$$

This does not rule out the cryosurface temperature or surface effects on the capture coefficient and applies only where the cryosurface temperature effects are constant or quite small in relation to the gas temperature effect. The values of ϵ/k and $(MV_{x_O}^2)/(2k)$ for each experimental gas were determined from the 300°K data using Eq. (7), and these values are given in Table 4. The capture coefficient for each gas was calculated from Eq. (7) for several gas temperatures, and one minus these values are represented by the solid lines in Figs. 17 and 18. The points in the figures are the experimental capture coefficients determined for a 20°K cryosurface for the indicated gases.

The deviation of the experimental capture coefficients from the values calculated from Eq. (7) for gas temperatures less than 300°K may be qualitatively explained by the potential well theory (Ref. 5). When a molecule approaches the cryosurface, it enters a potential field created by the condensate and is accelerated (Ref. 16). The magnitude of this change in velocity is dependent on three factors: (1) The strength of the potential field, which is a function of the cryosurface temperature and the species of the gas condensed, (2) the angle of approach of the molecule, and (3) the length of time the incident molecule is exposed to this potential field. The strength of the field and the angle of approach should be independent of the gas temperature; however, the length of time the approaching molecule spends in the field is dependent on its velocity or $(T_g)^{1/2}$. Therefore, the change in velocity would be greater for the 77°K molecules than for the 300°K molecules, and so forth. Then

the experimental capture coefficient would tend to be lower for the 77°K gas temperature experiments than those predicted from Eq. (7) because of the disturbance of the Maxwellian distribution by the potential field at the cryosurface. This effect would also explain the slight decrease in the capture coefficient for the 300°K gas temperature measurements observed when the cryosurface temperature is varied from 10 to 25°K.

In Fig. 19, the data points represented by triangular symbols are experimental values of the capture coefficient for carbon dioxide (CO_2) at gas temperatures of from 400 to 950°K obtained in the propulsion studies (Ref. 17). The good agreement between the experimental and calculated points indicates that the capture coefficient may be calculated with reasonable accuracy at these higher temperatures. However, the possible error involved in this type of extrapolation is shown in Fig. 20. The shaded portion represents the area where the actual values of C may fall. This area is based on a maximum error of ±8 percent in the 195, 300, and 400°K data. For N_2 and A, the possible error is increased since the 77°K points were not used in the extrapolation because of cryosurface temperature influences at 20°K.

It should be noted that if Eq. (7) is used to calculate capture coefficients for gas temperatures less than 300°K, the effects of cryosurface temperature must be considered.

6.0 CONCLUSIONS

The critical velocity model has been shown to predict the experimental results of capture coefficient measurements for gas temperatures ≥ 300°K, and the deviations from the predicted values can be qualitatively accounted for if the potential field model is employed. Therefore, one may estimate the capture coefficients for engineering purposes for most gases from Eq. (9), if the capture coefficient is known for one gas temperature:

$$(1 - C_1)^{T_1} = (1 - C_2)^{T_2} \tag{9}$$

where

$$T_1 \quad \text{and} \quad T_2 \geq 300°K$$

From the values of ϵ/k in Table 4, one may conclude that these gases will fall within one of two main groups. The factors that decide to which group a gas will belong have not been determined; however, it is felt that an explanation of the cryosurface temperature effect will elucidate these factors. The effects of cryosurface temperature are the subject of a continuing study (Ref. 4).

REFERENCES

1. Carlson, Lt. Col. Donald D., USAF, and Underwood, Robert H. "Design of an Aerospace Systems Environmental Chamber." AEDC-TR-61-10, July 1961.

2. Dawson, J. P. "Capture Coefficients of N_2-O_2 Mixtures." AEDC-TDR-64- (to be published).

3. Buffham, B. A., Henault, P. B., and Flinn, R. A. "A Theoretical Evaluation of the Sticking Coefficient in Cryopumping." Transactions of the Ninth Vacuum Symposium, G. N. Brancroft (ed.), 1962.

4. Collins, F. C. Chemistry Department, Brooklyn Polytechnic Institute, Private Communication.

5. Dawson, J. P. and Haygood, J. D. "Temperature Effects on the Capture Coefficient of CO_2." AEDC-TDR-63-251, January 1964.

6. Collins, J. A., Jr., and Dawson, J. P. "Cryopumping of 77°K Nitrogen and Argon on 10-25°K Surfaces." AEDC-TDR-63-51, May 1963.

7. Dawson, J. P., Haygood, J. D., and Collins, J. A., Jr. "Temperature Effects on the Capture Coefficients of CO_2, N_2, and A." Advances in Cryogenic Engineering, Vol. 8, K. D. Timmerhaus (ed.), Plenum Press, Inc., New York, 1963.

8. Jeans, J. Introduction to the Kinetic Theory of Gases. Cambridge University Press, 1960.

9. Haygood, J. D. and Dawson, J. P. "Fundamental Considerations in the Measurement of Capture Coefficients." AEDC-TDR-64- (to be published).

10. Wang, E. S. J., Collins, J. A., Jr., and Haygood, J. D. "General Cryopumping Study." Advances in Cryogenic Engineering, Vol. 7, K. D. Timmerhaus (ed.), Plenum Press, Inc., New York, 1962.

11. Dushman, S. Scientific Foundations of Vacuum Technique. J. M. Lafferty (ed.), John Wiley and Sons, Inc., New York, 1949 (Second Edition).

12. Honig, R. E. and Hook, H. O. "Vapor Pressure Data for Some Common Gases." RCA Review, Vol. XXI, No. 3, September, 1960, pp. 360-368.

13. Collins, J. A., Jr., Haygood, J. D., and Wang, E. S. J. "Initial Study of the Effect of Cryosurface Geometry on Cryopumping." AEDC-TDR-62-46, April 1962.

14. Wang, E. S. J., Collins, J. A., Jr., and Haygood, J. D. "Cryopumping in the Near Free-Molecule Flow Region." Advances in Cryogenic Engineering, Vol. 7, K. D. Timmerhaus (ed.), Plenum Press, Inc., New York, 1962.

15. Moelwyn-Hughes, E. A. Physical Chemistry. Pergamon Press, New York, 1957.

16. Kirkwood, J. G. and Buff, F. P. "The Statistical Mechanical Theory of Surface Tension." Journal of Chemical Physics, Vol. 17, March 1949, pp. 338-343.

17. McCullough, B. A. and Wang, E. S. J. "Cryopumping of CO_2 Nozzle Flow by 77°K Cryosurface." AEDC-TDR-64- (to be published).

TABLE 1

MINIMUM PRESSURES ATTAINED IN THE ULTRAHIGH VACUUM CHAMBER

Major Gas Present	System Pressure, mm Hg	Diffusion Pump	VacIon Pump	Cryosurface Temperature	Wall Temperature
CO	2×10^{-10}	On	On	Ambient	Ambient
CO	3×10^{-10}	On	Off	"	"
CO	2×10^{-10}	Off	On	"	"
A	4×10^{-10}	On	On	"	"
N_2	2×10^{-10}	On	On	"	"
N_2	1.5×10^{-11}	Off	Off	10°K	"
N_2	1×10^{-11}	Off	Off	"	77°K
N_2O	1×10^{-11}	Off	Off	"	300°K
A	2.8×10^{-11}	Off	Off	"	"
CO	2.2×10^{-11}	Off	Off	"	"

TABLE 2

PUMPING SPEEDS OF COMMON GASES

Cryosurface Temperature, °K	Pumping Speed, S, liters/cm^2-sec											
	N_2		A		CO			N_2O		O_2*		
	300°K	400°K	300°K	400°K	77°K	300°K	400°K	300°K	400°K	77°K	300°K	400°K
10	7.75	6.53	6.80	5.76	6.04	10.5	10.0	5.95	4.8			
12.5	7.65	6.53	6.75	5.76	6.04	10.1	10.0	5.95	4.8			
15	7.55	6.53	6.65	5.66	6.04	10.0	10.0	5.95	4.8			
17.5	7.4	6.53	6.55	5.66	6.04	10.0	10.0	5.95	4.8			
20	7.35	6.53	6.50	5.66	6.04	10.0	10.0	5.95	4.8	5.36	8.77	8.9
22.5	7.30	6.53	6.50	5.66	6.04	10.0	10.0	5.95	4.8			
25	7.30	6.53	6.50	5.66	6.04	10.0	10.0	5.95	4.8			

*Estimated (Ref. 2)

TABLE 3

THEORETICAL MAXIMUM PUMPING SPEEDS

Gas	Molecular Weight, M, grams	Gas Temperature, T_g, °K	Maximum Pumping Speed, S, liters/cm^2-sec
N_2, CO	28	77	6.04
	28	300	11.96
	28	400	13.8
O_2	32	77	5.36
	32	300	10.58
	32	400	12.2
A	40	77	5.06
	40	300	10.00
	40	400	11.55
CO_2, N_2O	44	195	7.68
	44	300	9.53
	44	400	11.02

TABLE 4

CALCULATED VALUES OF ϵ/k

Gas	ϵ/k*
N_2	290
A	293
CO_2	289
CO	532
N_2O	288
O_2	532

*These values of ϵ/k were calculated from the 300°K gas temperature data, measured on a 20°K cryosurface.

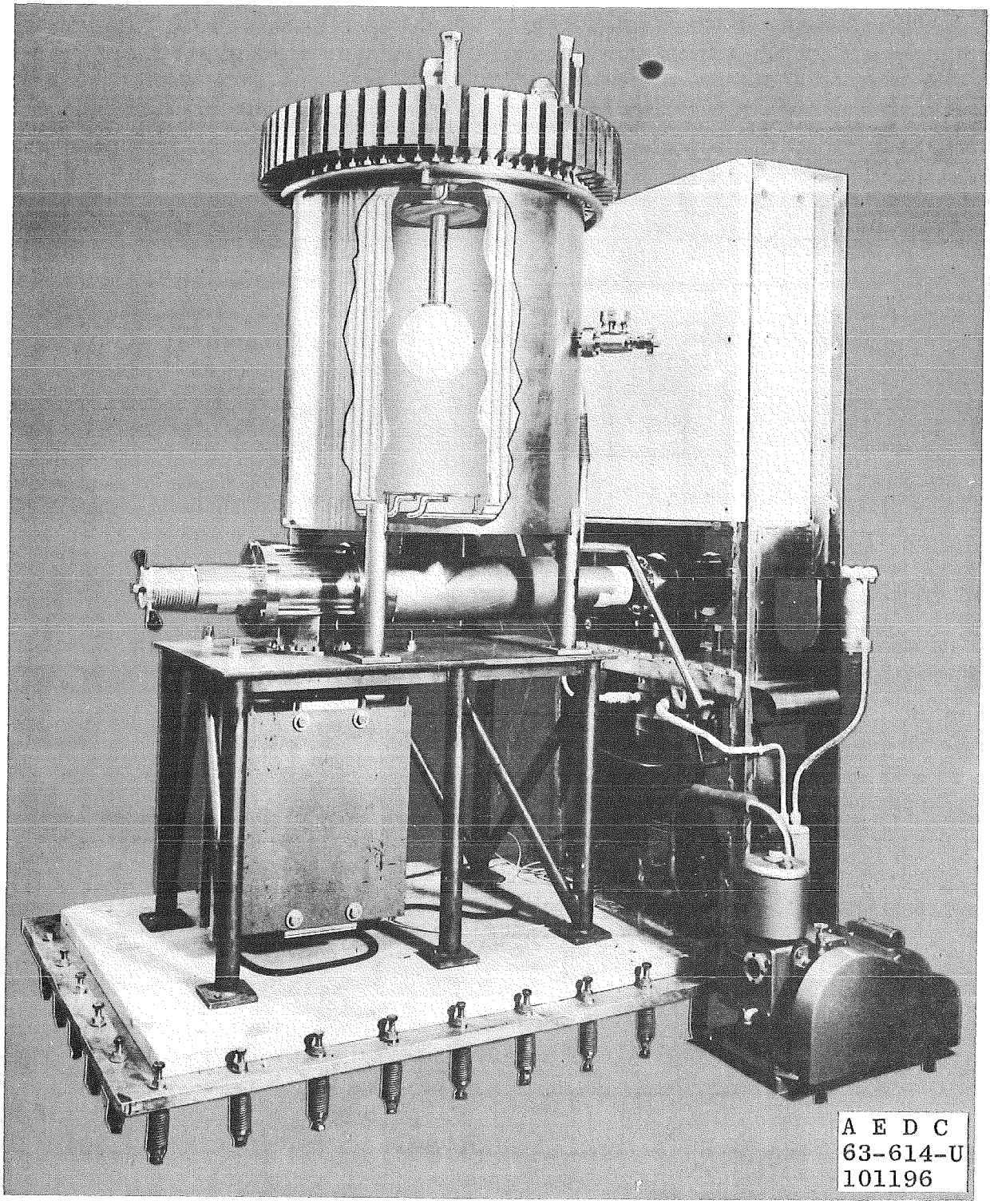

Fig. 1 Ultrahigh Vacuum Chamber

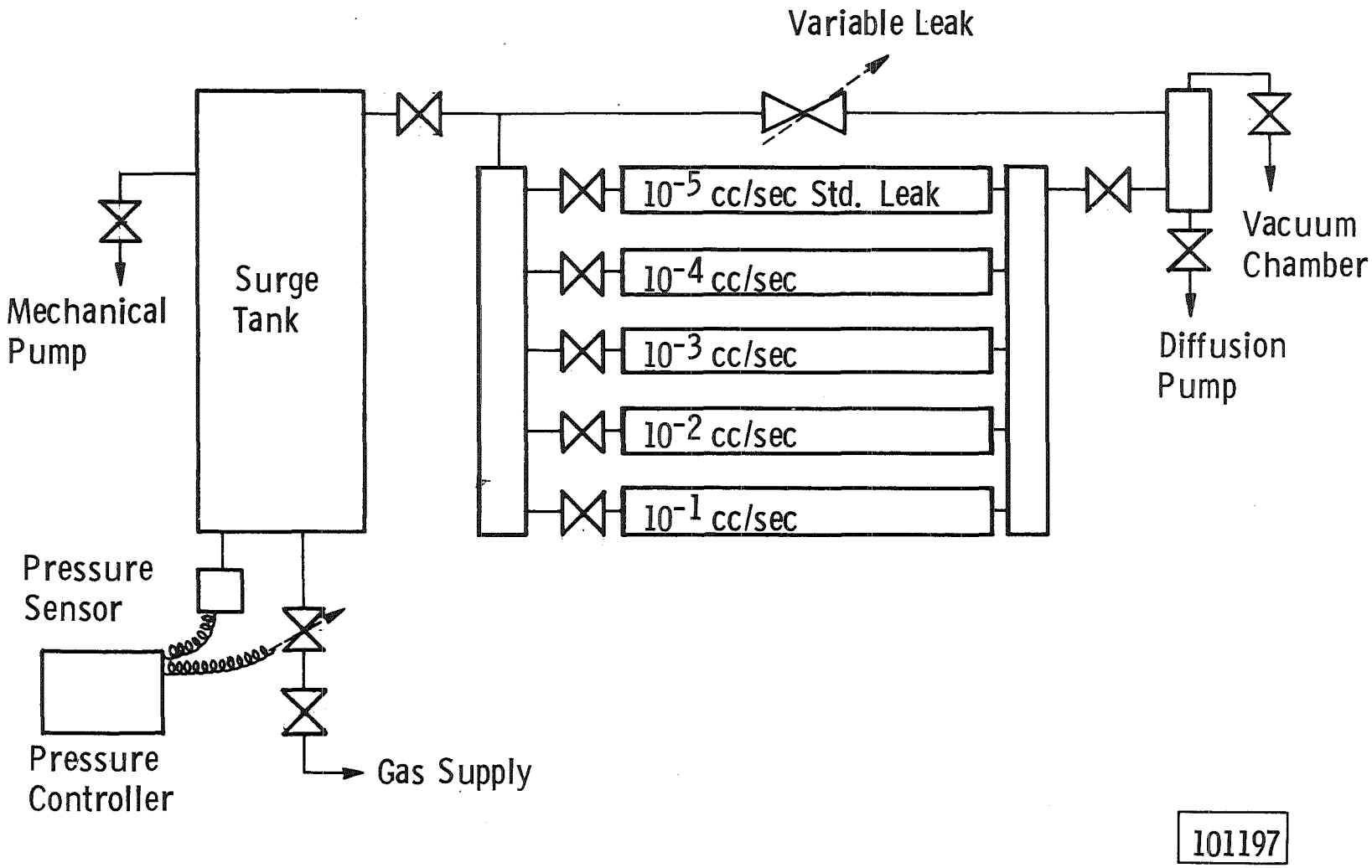

Fig. 2 Gas Addition System

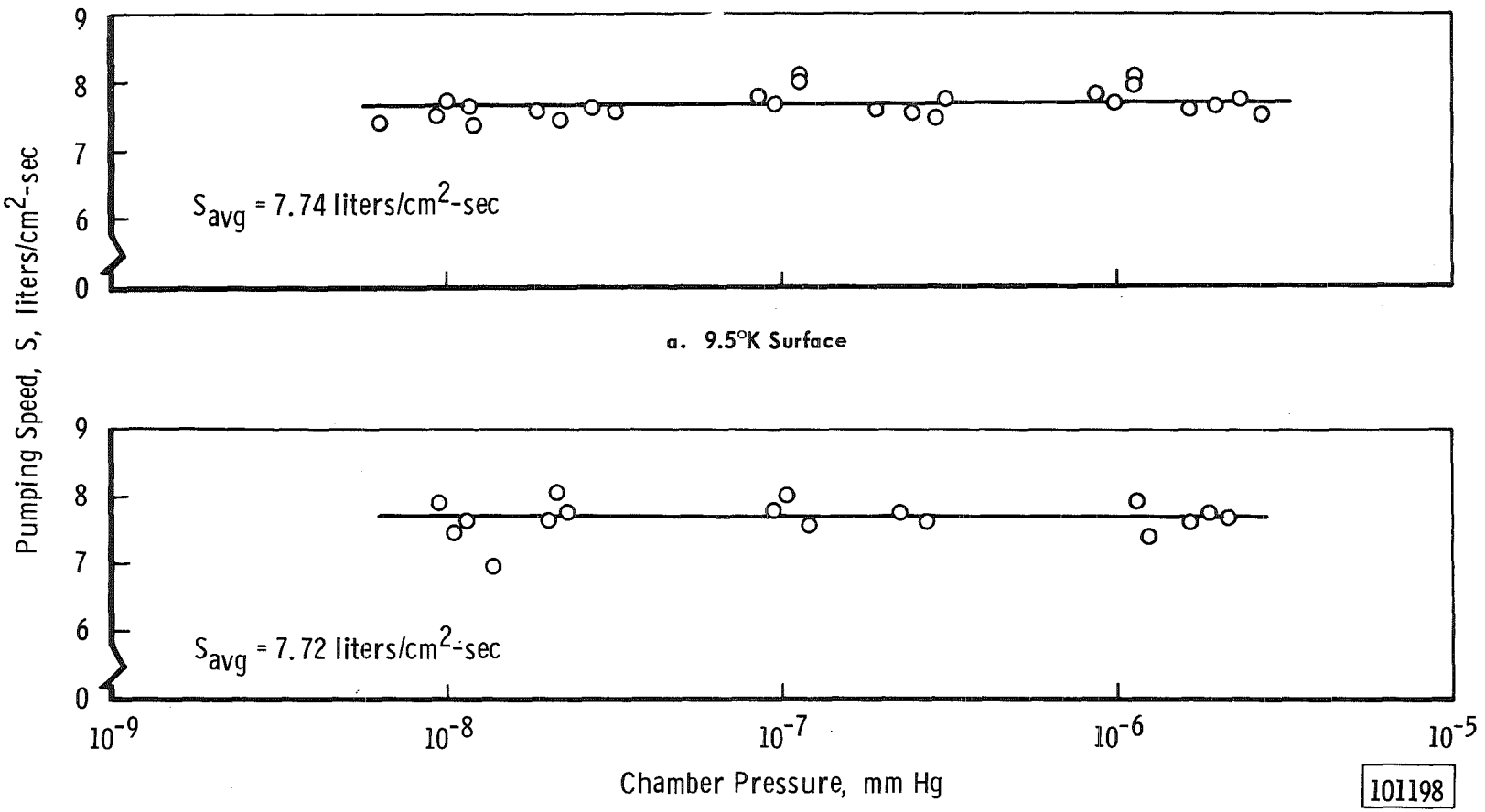

a. 9.5°K Surface

b. 10.5°K Surface

Fig. 3 Pumping Speeds for 300°K Nitrogen

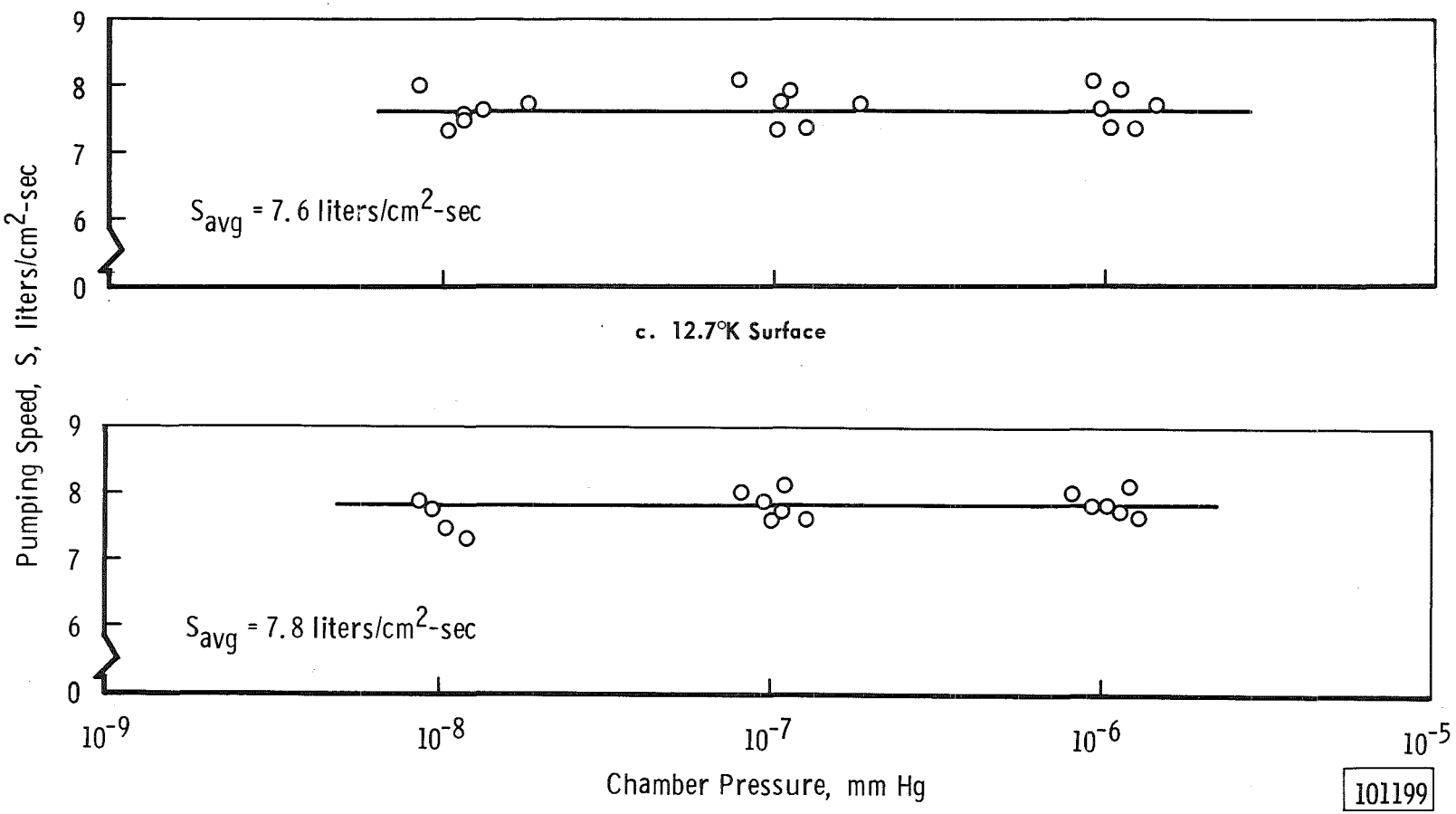

c. 12.7°K Surface

d. 14.1°K Surface

Fig. 3 Continued

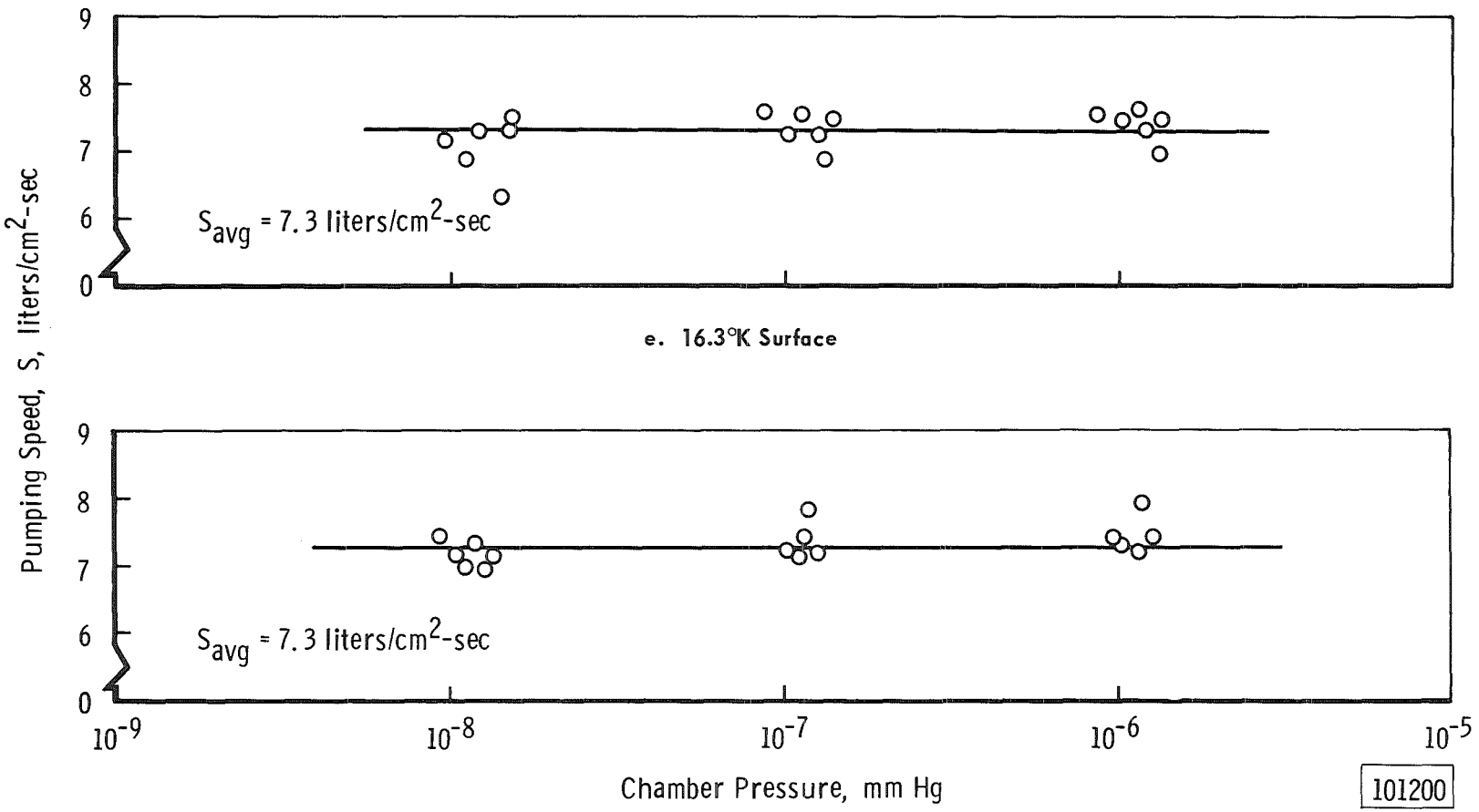

e. 16.3°K Surface

f. 18.4°K Surface

Fig. 3 Continued

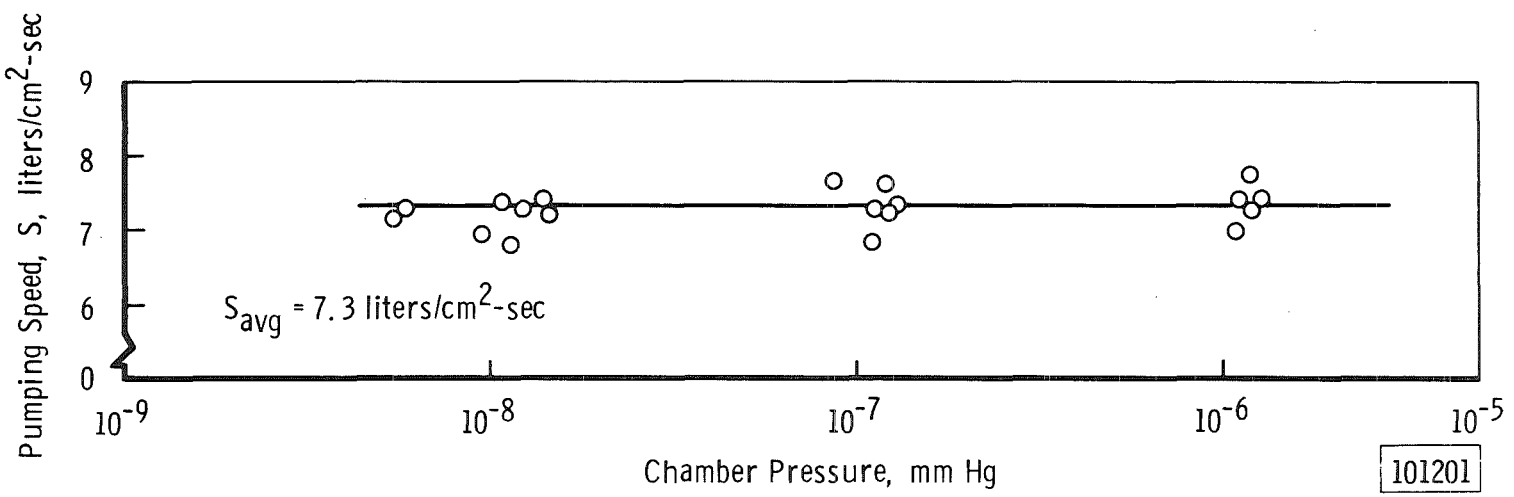

g. 22.6°K Surface

Fig. 3 Concluded

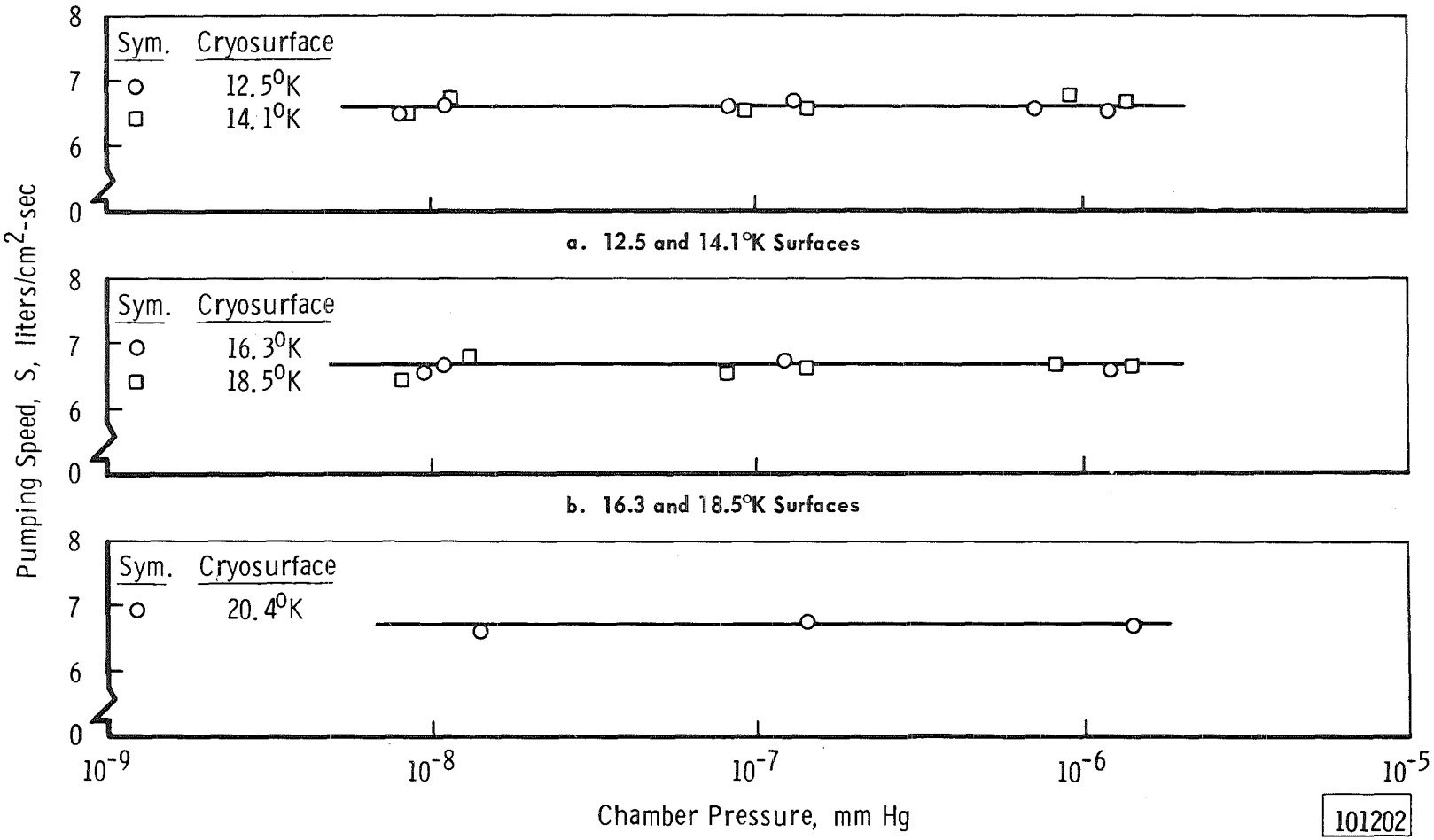

a. 12.5 and 14.1°K Surfaces

b. 16.3 and 18.5°K Surfaces

c. 20.4°K Surface

Fig. 4 Pumping Speeds for 400°K Nitrogen

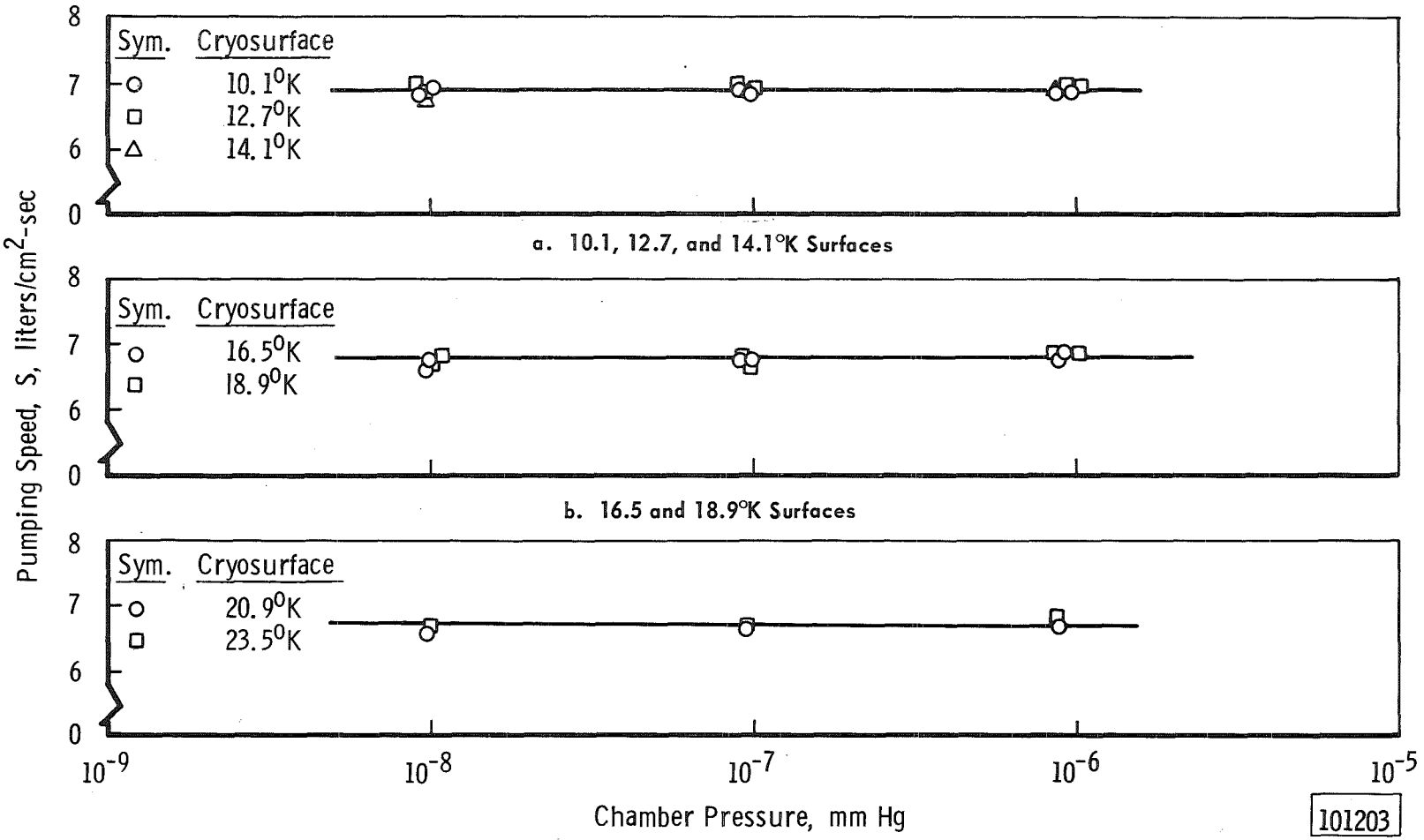

a. 10.1, 12.7, and 14.1°K Surfaces

b. 16.5 and 18.9°K Surfaces

c. 20.9 and 23.5°K Surfaces

Fig. 5 Pumping Speeds for 300°K Argon

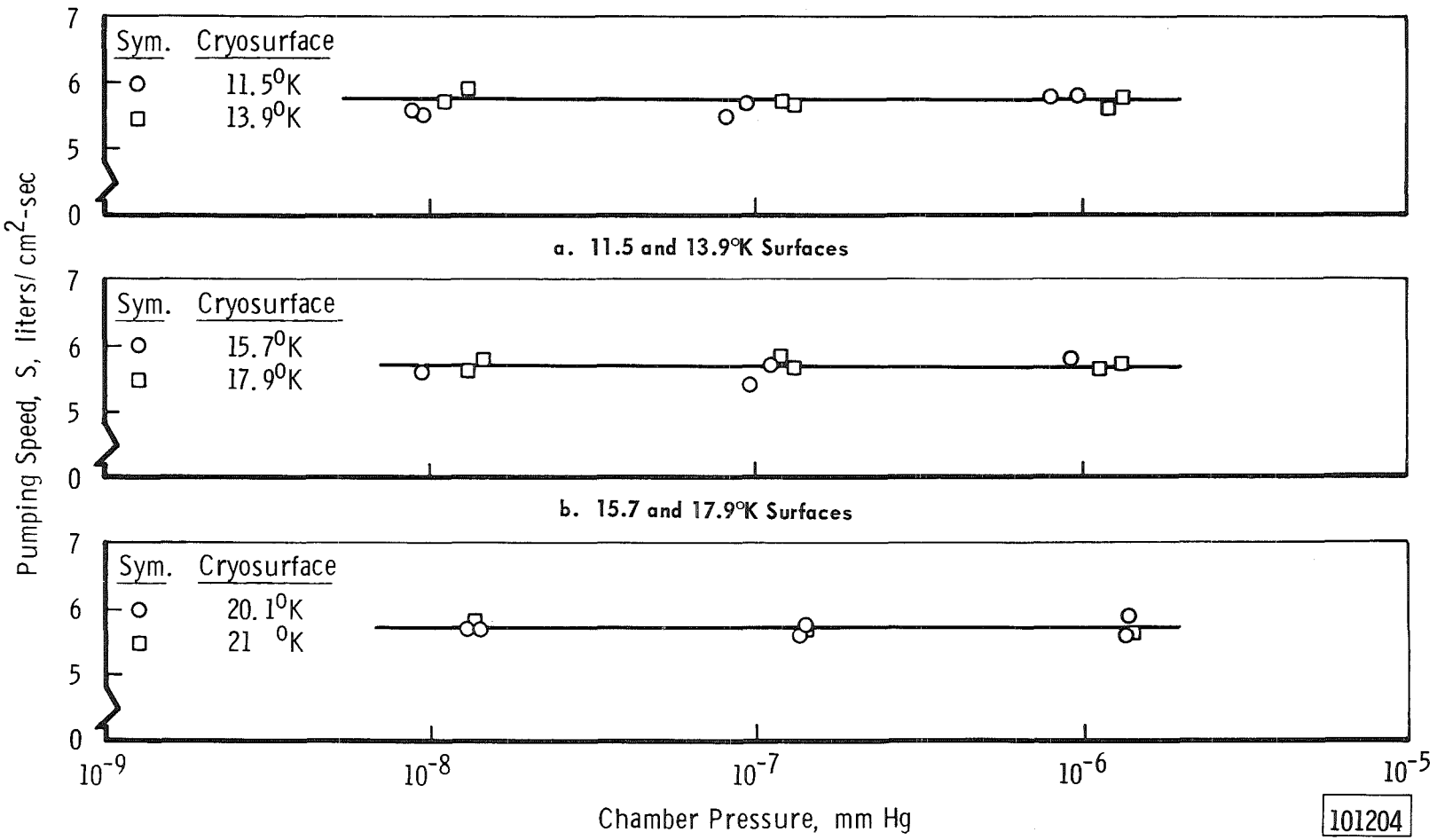

a. 11.5 and 13.9°K Surfaces

b. 15.7 and 17.9°K Surfaces

c. 20.1 and 21°K Surfaces

Fig. 6 Pumping Speeds for 400°K Argon

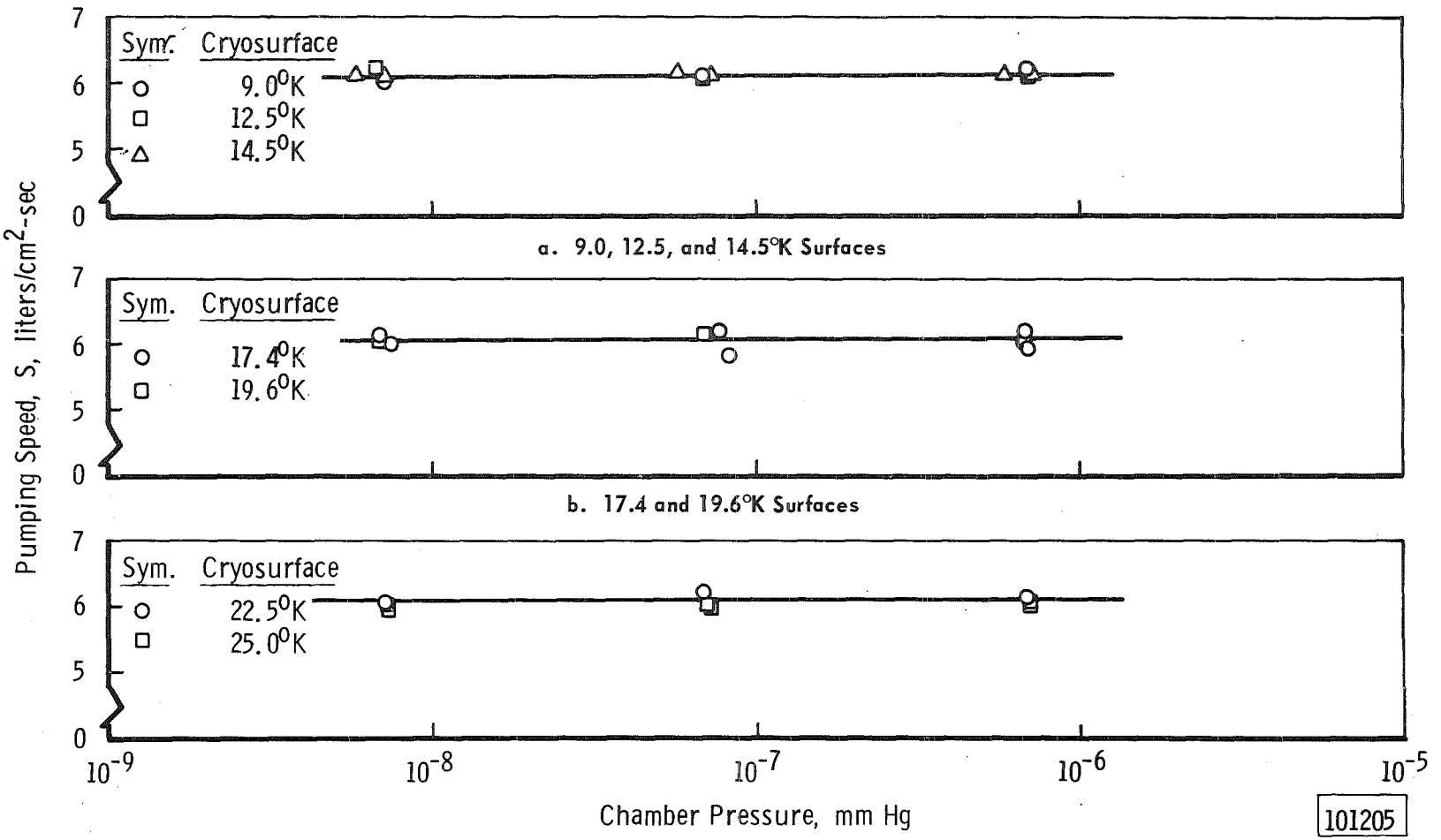

a. 9.0, 12.5, and 14.5°K Surfaces

b. 17.4 and 19.6°K Surfaces

c. 22.5 and 25°K Surfaces

Fig. 7 Pumping Speeds for 77°K Carbon Monoxide

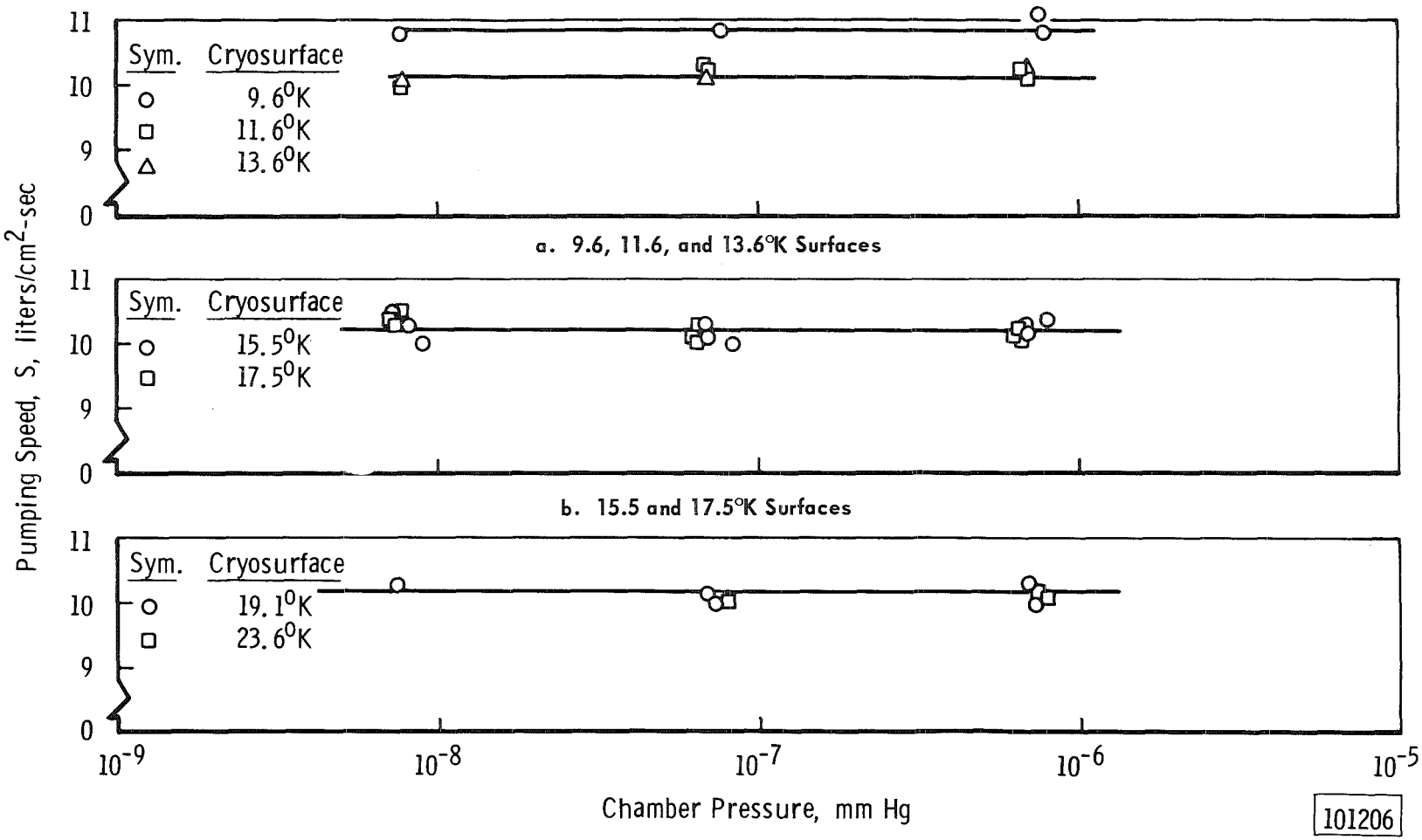

a. 9.6, 11.6, and 13.6°K Surfaces

b. 15.5 and 17.5°K Surfaces

c. 19.1 and 23.6°K Surfaces

Fig. 8 Pumping Speeds for 300°K Carbon Monoxide

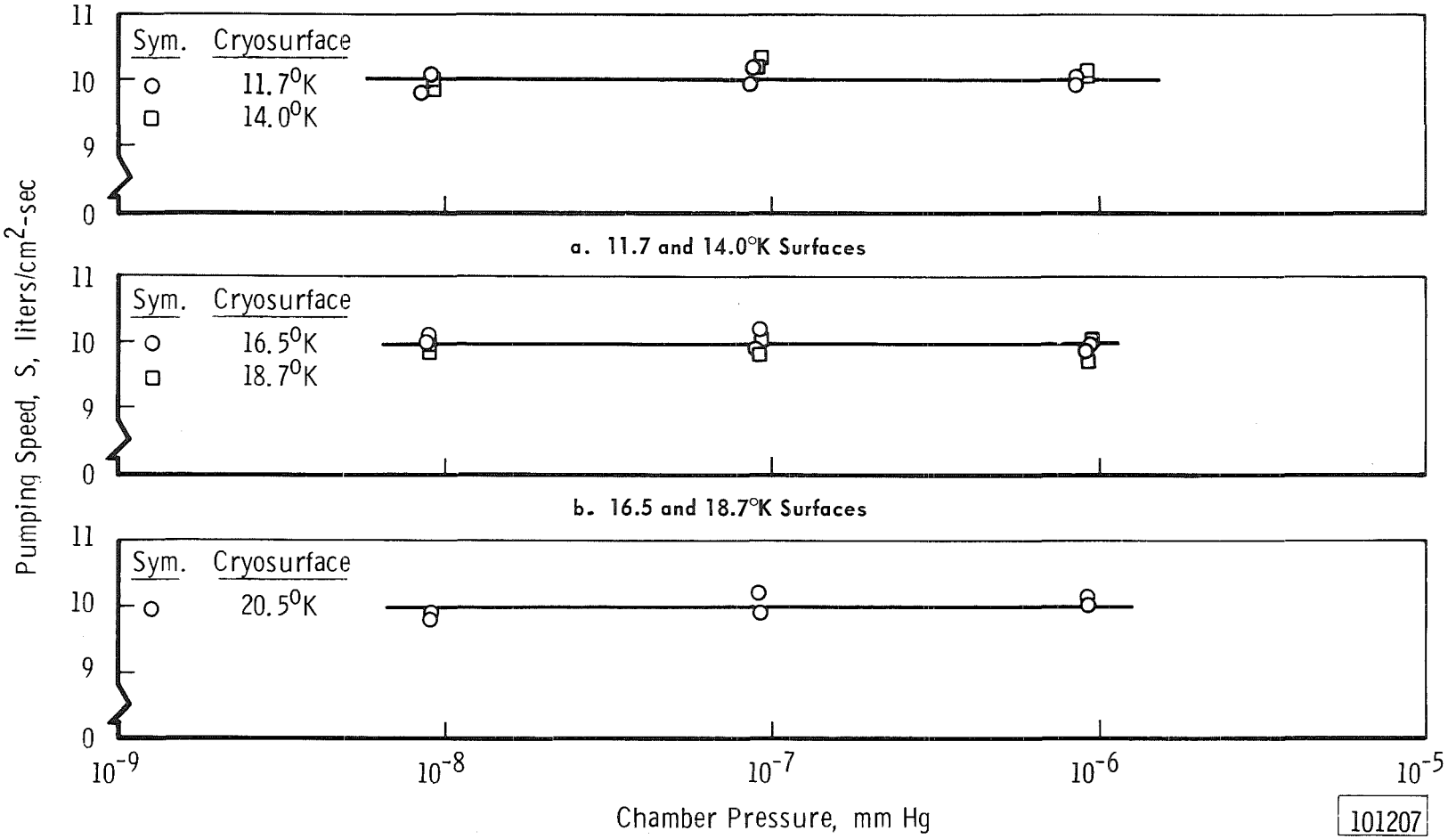

a. 11.7 and 14.0°K Surfaces

b. 16.5 and 18.7°K Surfaces

c. 20.5°K Surfaces

Fig. 9 Pumping Speeds for 400°K Carbon Monoxide

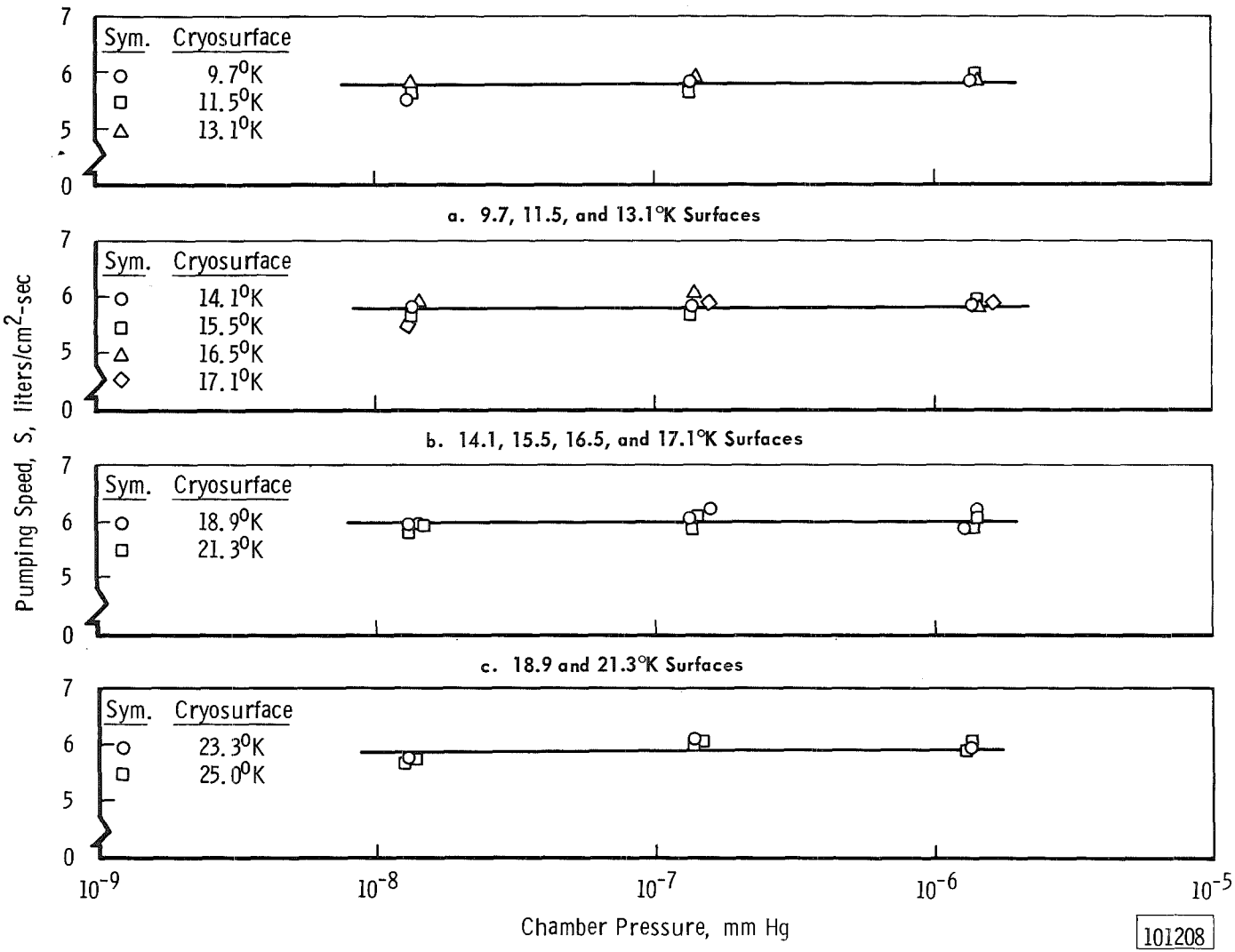

a. 9.7, 11.5, and 13.1°K Surfaces

b. 14.1, 15.5, 16.5, and 17.1°K Surfaces

c. 18.9 and 21.3°K Surfaces

d. 23.3 and 25°K Surfaces

Fig. 10 Pumping Speeds for 300°K Nitrous Oxide

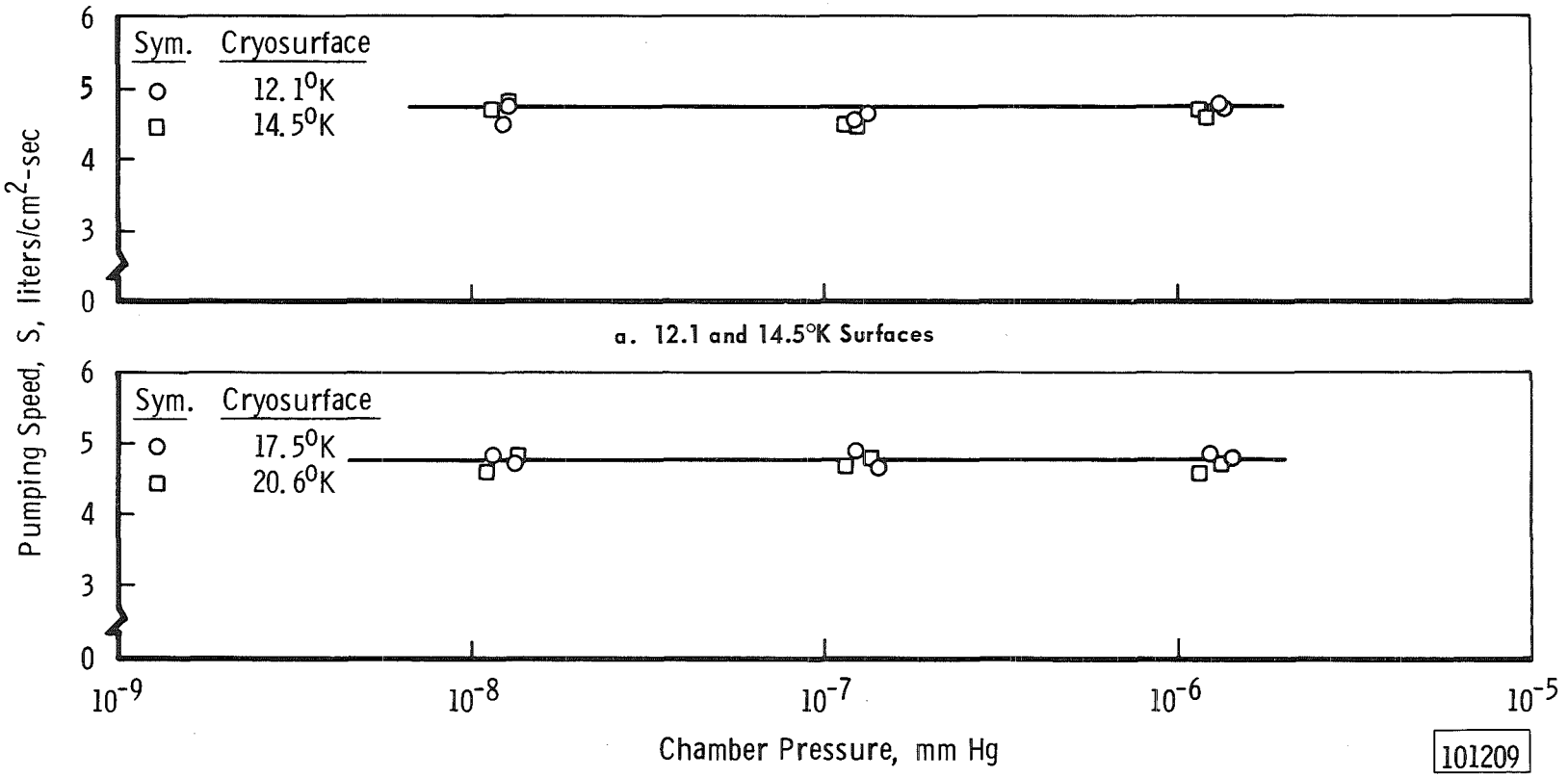

a. 12.1 and 14.5°K Surfaces

b. 17.5 and 20.6°K Surfaces

Fig. 11 Pumping Speeds for 400°K Nitrous Oxide

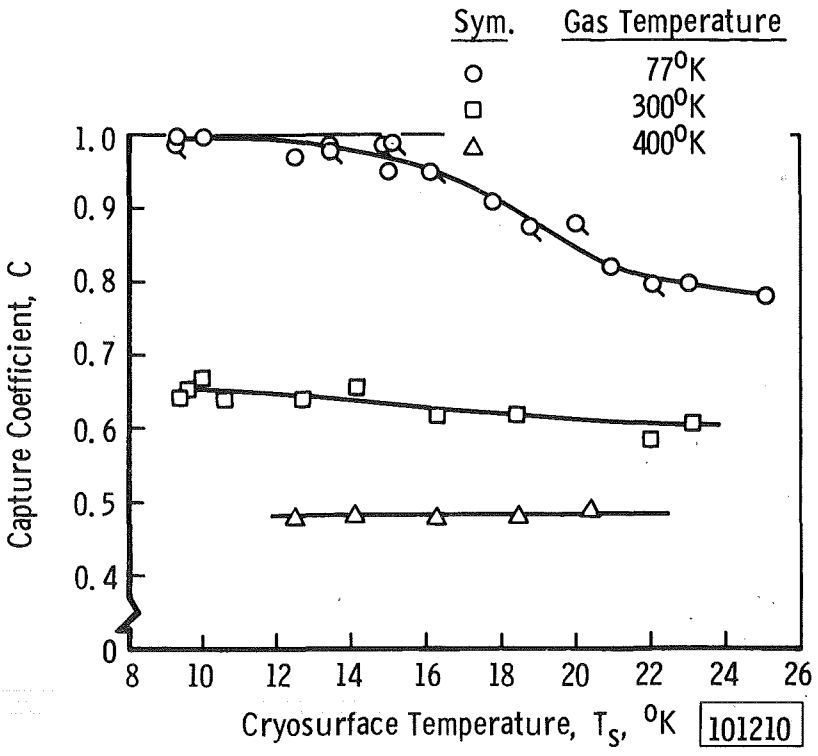

Fig. 12 Capture Coefficients of Nitrogen

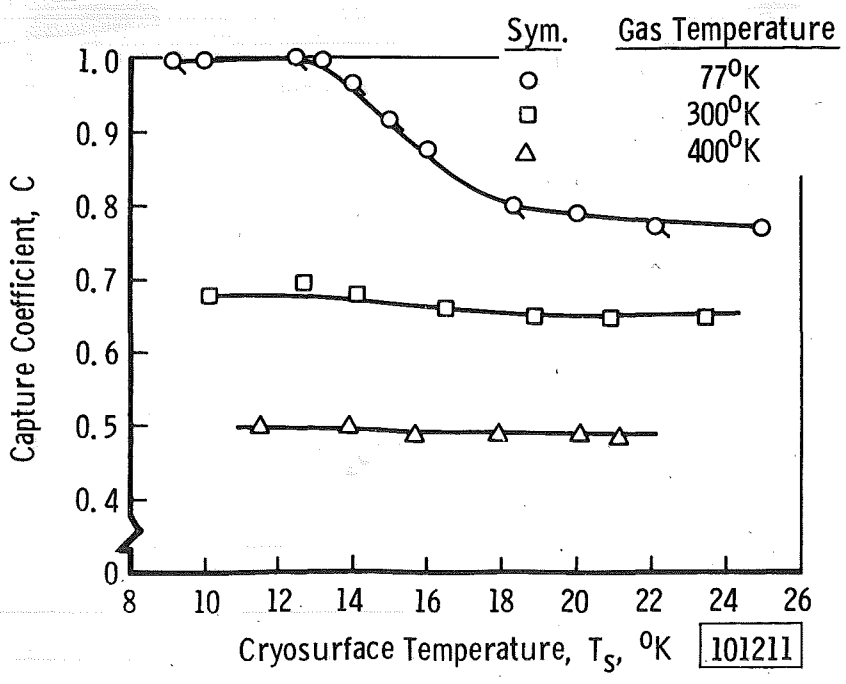

Fig. 13 Capture Coefficients of Argon

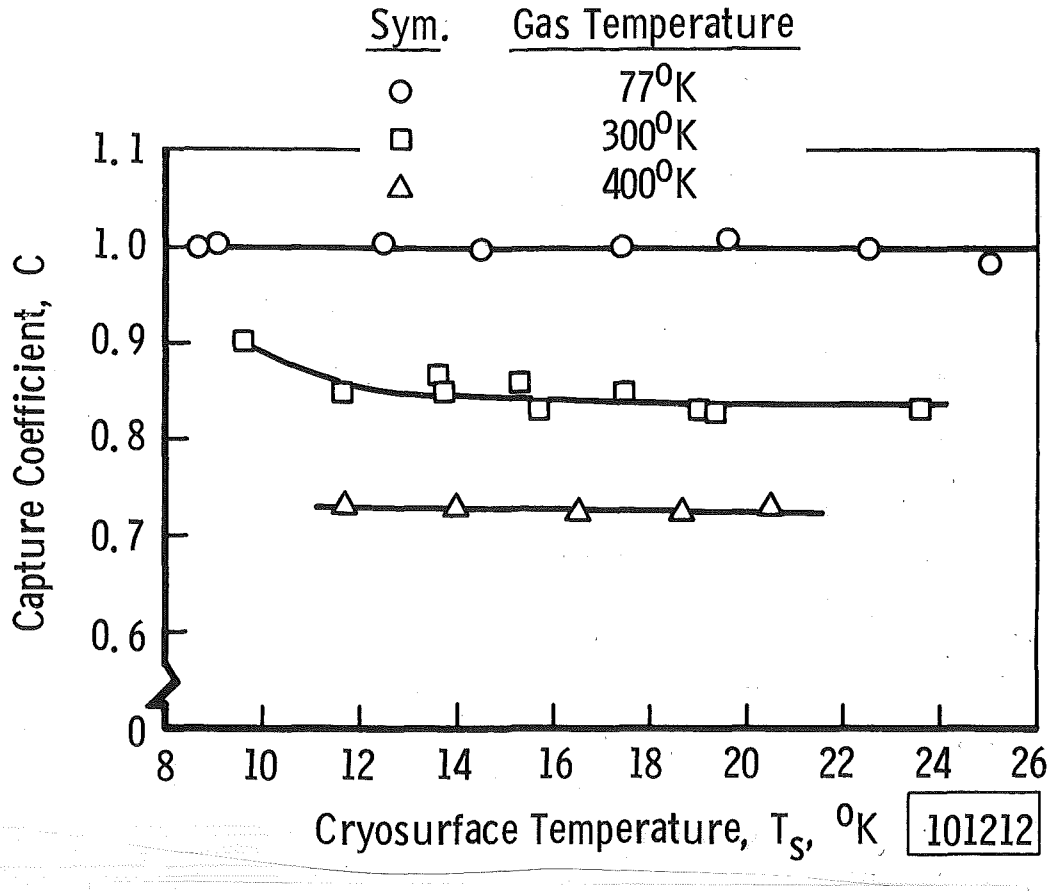

Fig. 14 Capture Coefficients of Carbon Monoxide

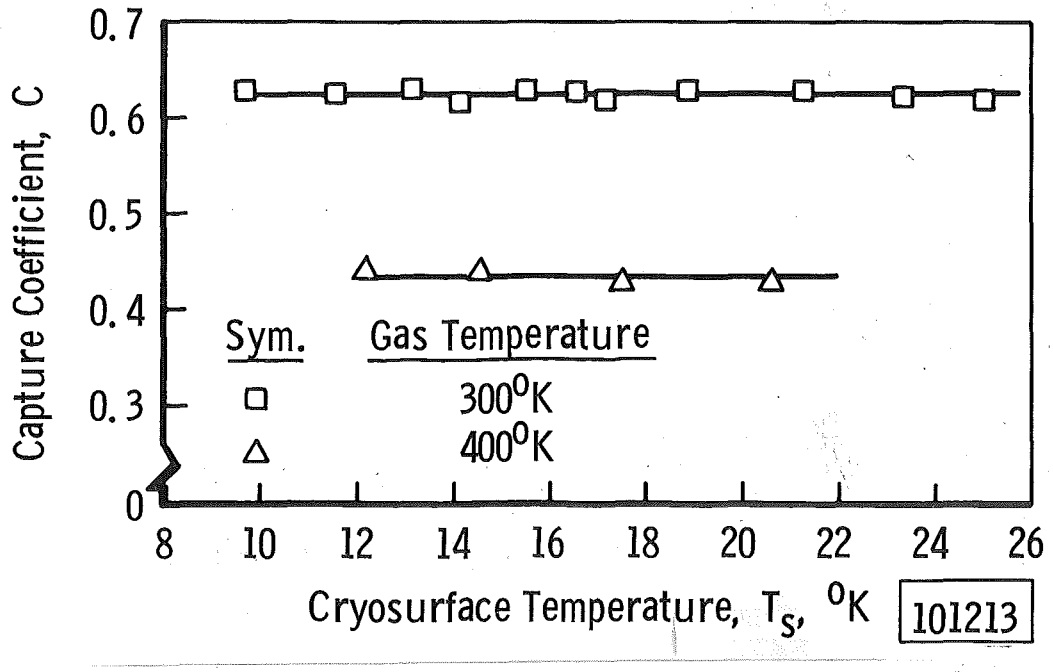

Fig. 15 Capture Coefficients of Nitrous Oxide

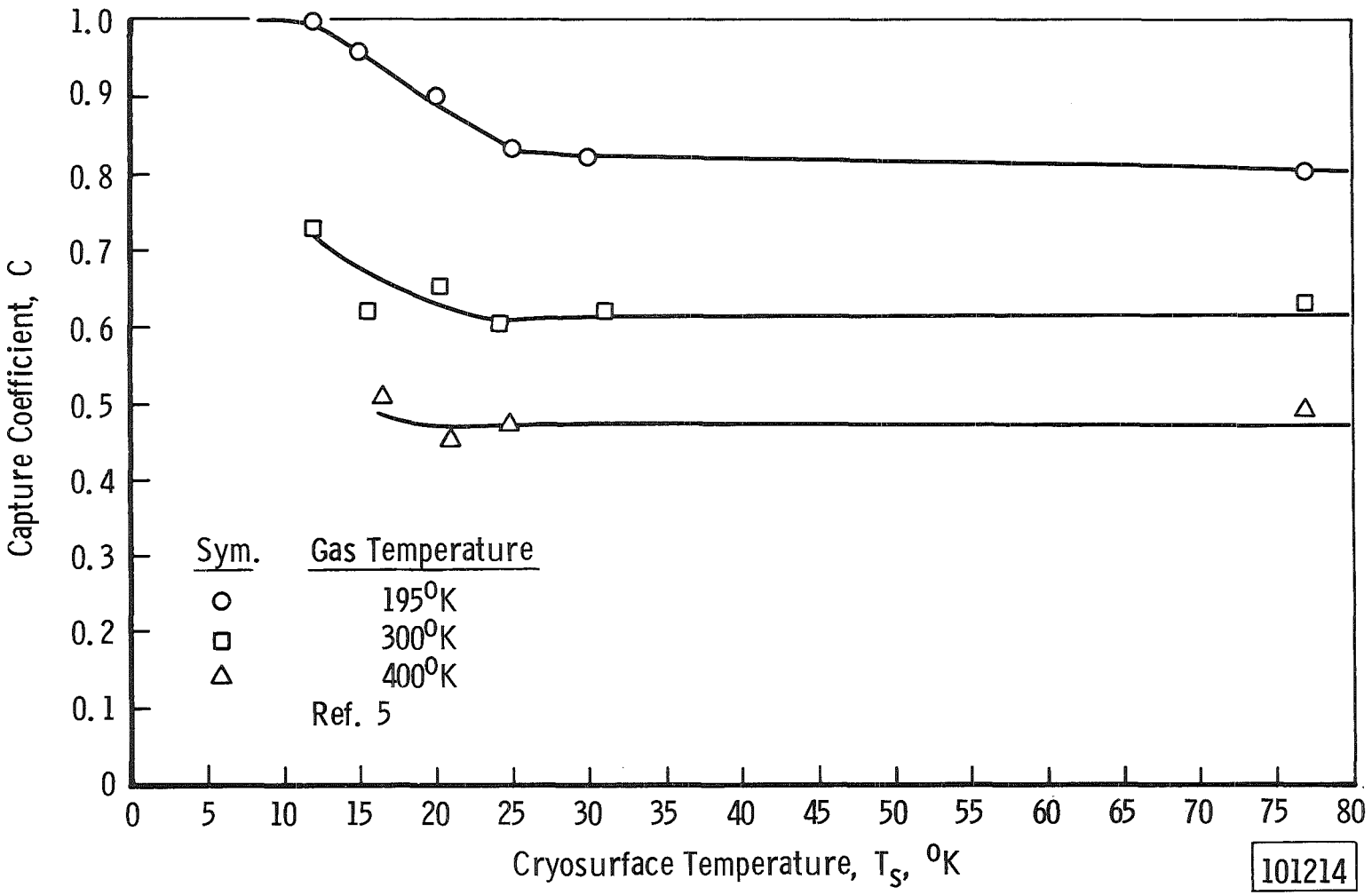

Fig. 16 Capture Coefficients of Carbon Dioxide

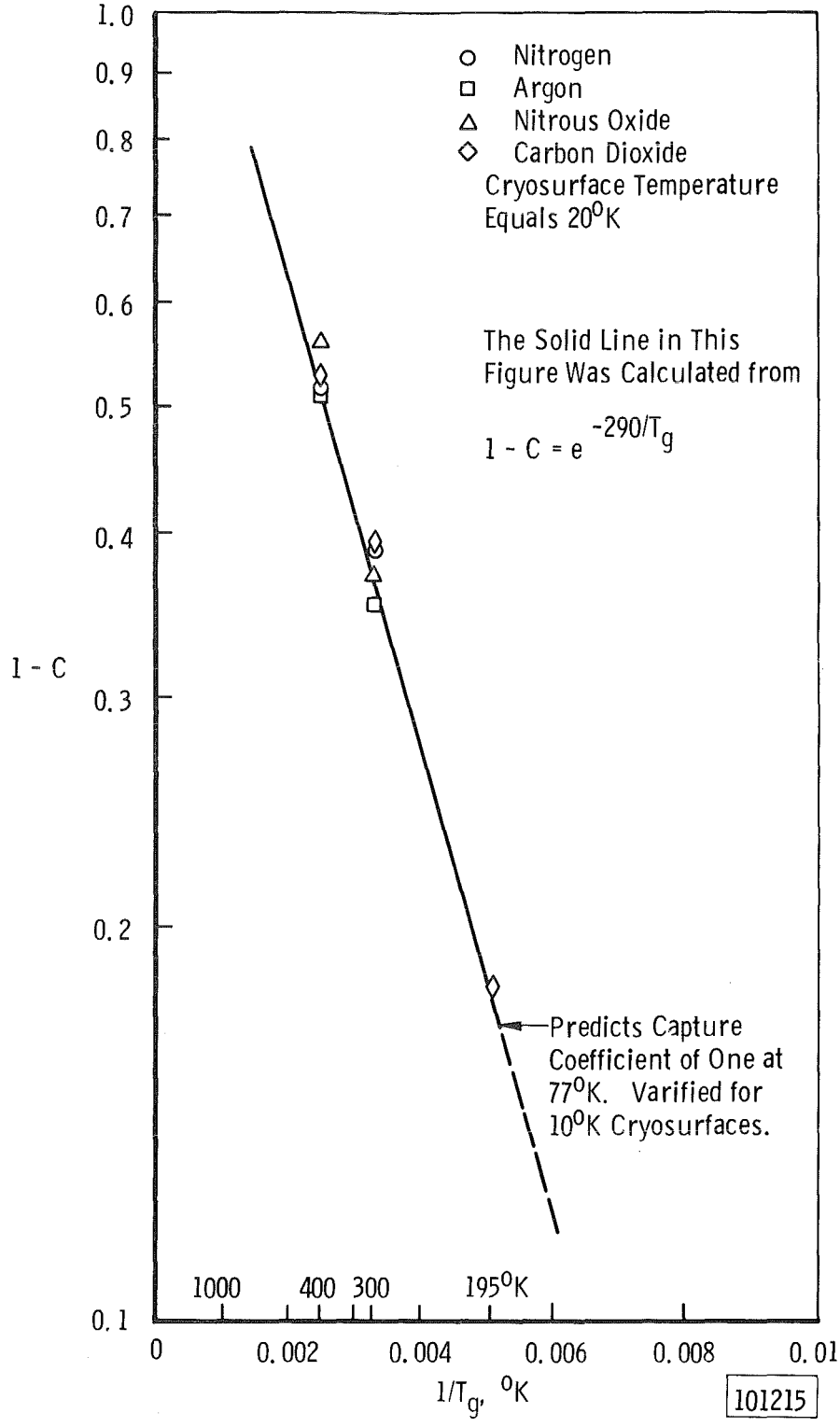

Fig. 17 Capture Coefficients as a Function of Gas Temperature for Nitrogen, Argon, Carbon Dioxide, and Nitrous Oxide

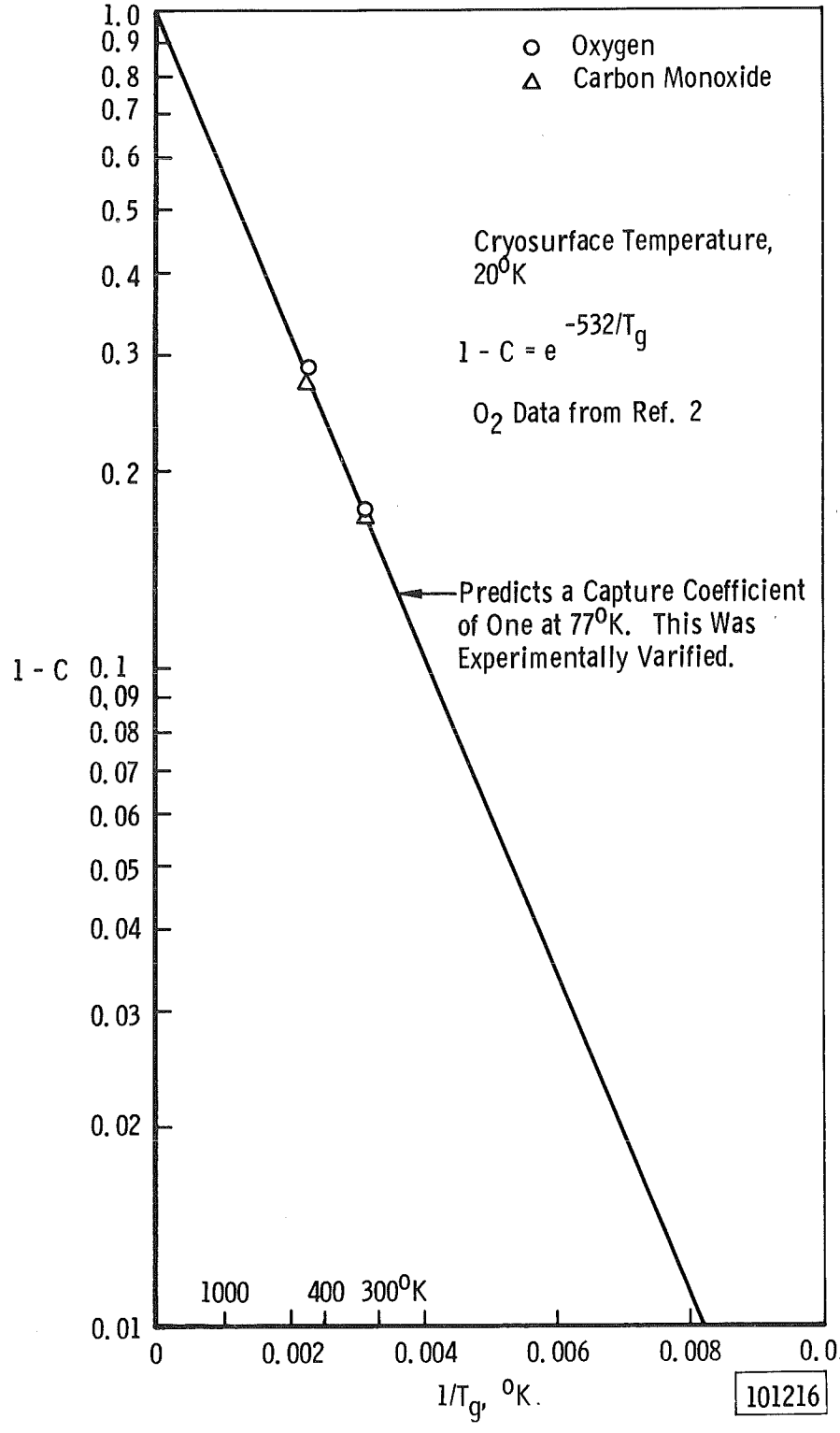

Fig. 18 Capture Coefficients as a Function of Gas Temperature for Oxygen and Carbon Monoxide

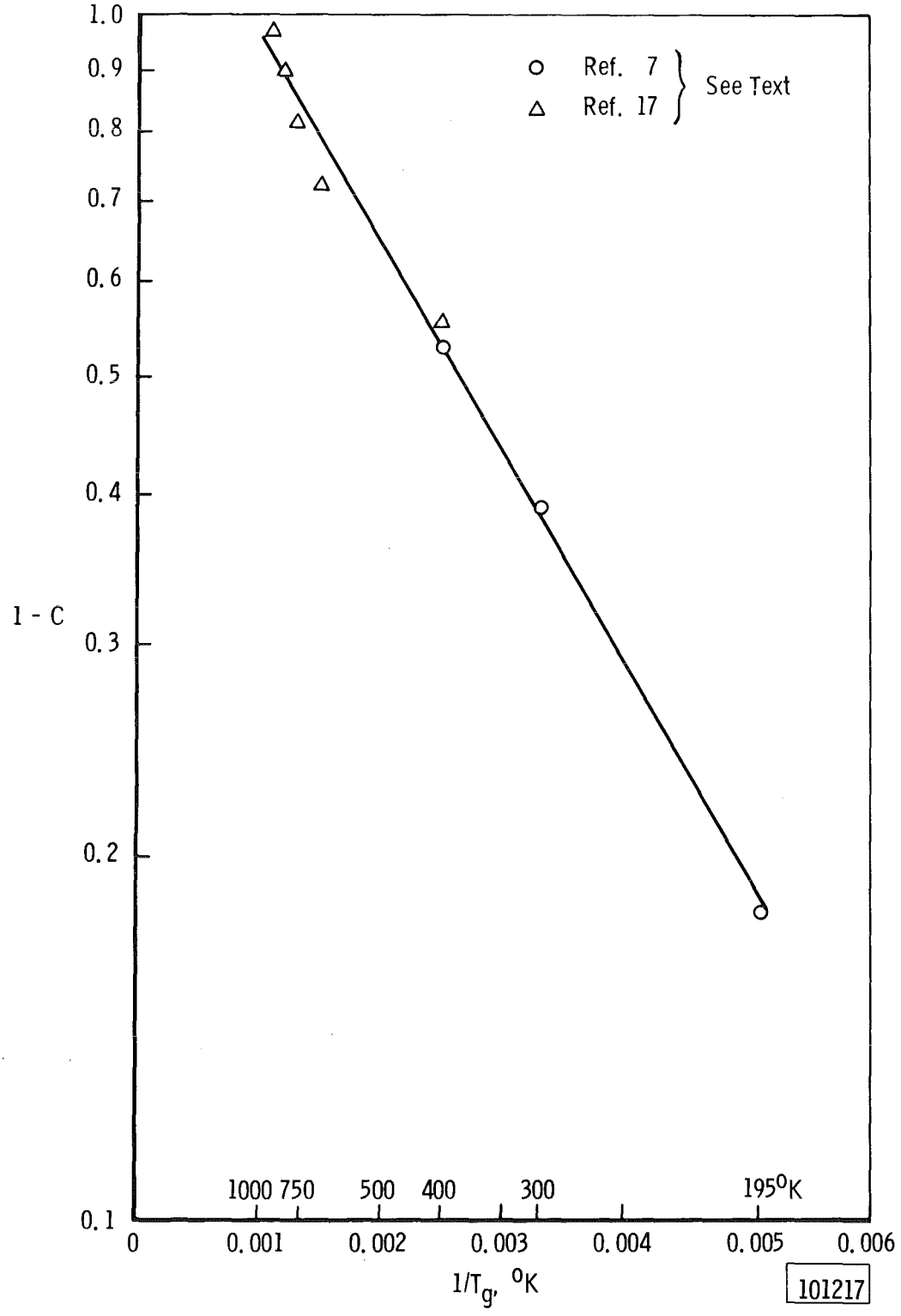

Fig. 19 Extrapolated Capture Coefficients of Carbon Dioxide

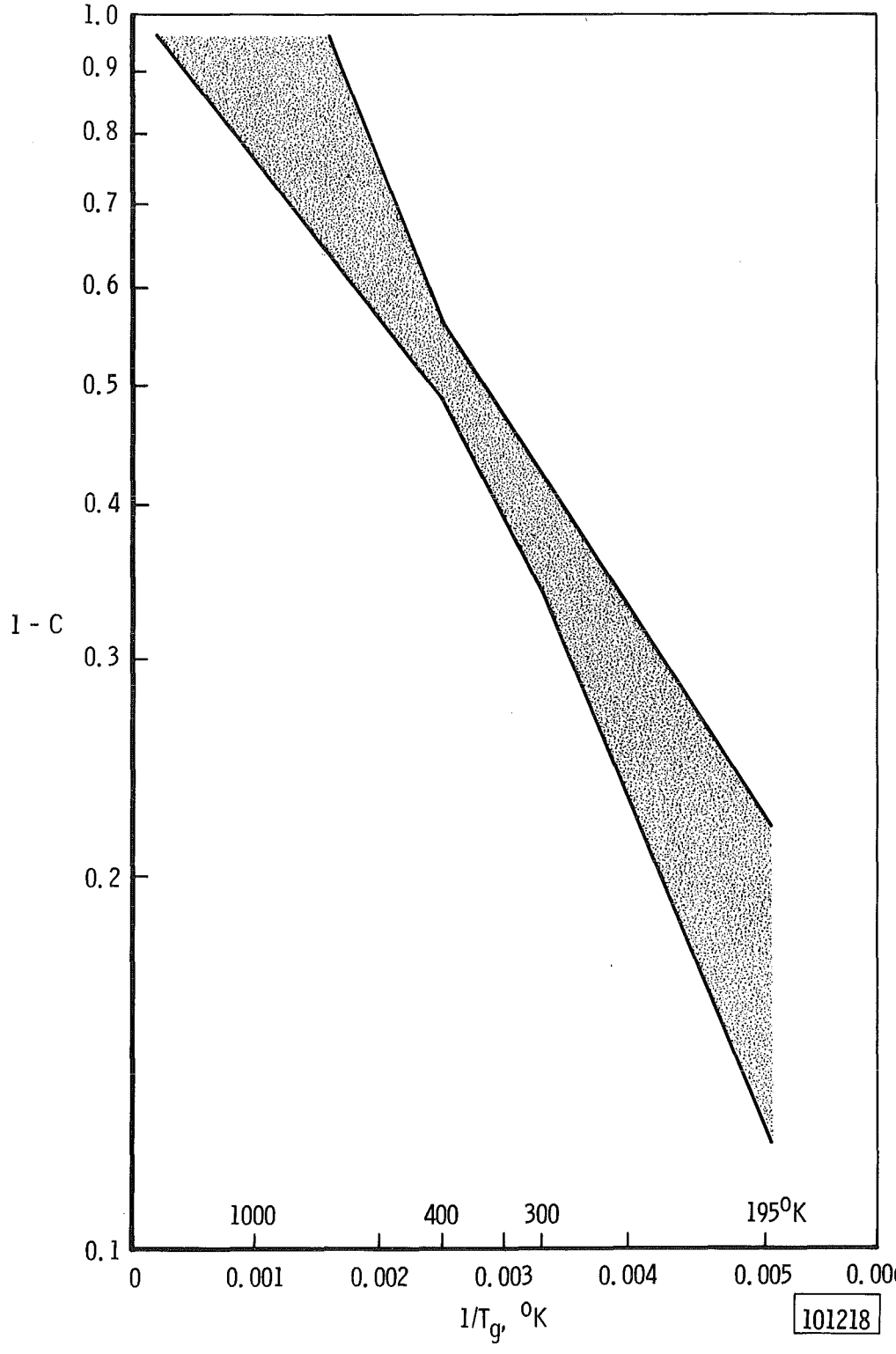

Fig. 20 Possible Experimental Error